ARMY RESEARCH LABORATORY

A Ballistic Compressor-Based Setup for the Visualization of Liquid Propellant Jet Combustion Above 100 MPa

by Avi Birk
and Douglas E. Kooker

ARL-TR-1490 September 1997

19971007 152

DTIC QUALITY INSPECTED 4

Approved for public release; distribution is unlimited.

The findings in this report are not to be construed as an official Department of the Army position unless so designated by other authorized documents.

Citation of manufacturer's or trade names does not constitute an official endorsement or approval of the use thereof.

Destroy this report when it is no longer needed. Do not return it to the originator.

Army Research Laboratory
Aberdeen Proving Ground, MD 21005-5066

ARL-TR-1490 **September 1997**

A Ballistic Compressor-Based Setup for the Visualization of Liquid Propellant Jet Combustion Above 100 MPa

Avi Birk, Douglas E. Kooker
Weapons and Materials Research Directorate

Approved for public release; distribution is unlimited.

Abstract

This report describes the components and operation of an experimental setup for the visualization of liquid propellant (LP) jet combustion at pressures above 100 MPa. The apparatus consists of an in-line ballistic compressor and LP injector. The ballistic compressor, based on a modified 76-mm gun, provides high-pressure (55 MPa) clear hot gas for the jet ignition. A piston (projectile) is fired toward a test chamber beyond the barrel's end, and its rebound is arrested in a transition section between the test chamber and the barrel. The LP jet is injected once the piston is restrained, and combustion of the jet further elevates the pressure. At a preset pressure, a disk in the piston ruptures, and the combustion gas vents sonically into the barrel. If a monopropellant is used, the jet injection-combustion process then resembles liquid rocket combustion, but at very high pressures (140 MPa). This report discusses the ballistics of the compression and compares experimental results to those predicted by a numerical model of the apparatus. Experimentally, a pressure of 70 MPa was achieved upon a 12.5 volumetric compression factor by firing a 10-kg piston into 1.04-MPa argon, using a charge of 75 g of small-grain M1 propellant.

Acknowledgment

The authors thank Dr. M. McQuaid of the U.S. Army Research Laboratory (ARL) for his involvement in the development of the wide-angle optics used for the visualization in the experimental setup.

INTENTIONALLY LEFT BLANK.

Table of Contents

INTENTIONALLY LEFT BLANK.

List of Figures

INTENTIONALLY LEFT BLANK.

1. Introduction

1.1 Background. A regenerative injection of liquid propellant (LP) has been the primary design approach for liquid gun propulsion [1] in the last 20 yr. This approach involves the high-pressure combustion of high-velocity-thick LP jets—a poorly understood process. To date, interior ballistic modeling has successfully simulated only mean pressures in gun fixtures, but not the high-frequency pressure fluctuations that plague the guns at pressures above 70 MPa. Gun developmental efforts culminated when an advanced 155-mm howitzer (Crusader) was constructed and extensively tested. Unfortunately, these efforts terminated by the end of FY96 because of persistent technical problems. Prominent among them were spiked ignition and pressure fluctuations during combustion. Despite the demise of the LP howitzer, the regenerative injection concept is now being considered for a gun in a future combat vehicle. An important item within the framework of a "Tech Base" program is the combustion research of LP jets at pressures above 70 MPa. The present research involves the visualization of LP jet combustion at high pressure, and it requires a novel experimental approach that is discussed herein. The hope is that the visualization data will provide flame stand-off distances for formulating realistic LP jet breakup and combustion algorithms applicable to the high-pressure regime where pressure fluctuations persist. We do not discuss, here, LP injection and combustion visualization data; rather we concentrate on the innovative aspects of the ballistic control of the experiment. In essence, we devised a method to generate a trapped volume of high-temperature and high-pressure nonvitiated test gas that can be used for LP ignition (as we do) or conceivably for other experiments involving fluids.

1.2 The Experimental Challenge. The construction of a test apparatus that provides adequate optical access to jet combustion at gun pressures is highly challenging. Baier [2] attempted to visualize jet combustion in an actual gun fixture, but the phenomena of interest were largely obscured by the optically thick and luminous igniter products. To overcome these obstacles, early laboratory-scale experiments with LP sprays in a windowed test chamber were conducted by Birk and Reeves [3] and later by Lee, Tseng, and Faeth [4]. In both efforts, LP was injected at velocities of 50 to 100 m/s into an environment conditioned by the combustion of a stoichiometric gas mixture.

The ambient gas temperature achieved in these experiments was close to the adiabatic flame temperature of the propellant. However, observations were limited to pressures below 9 MPa because, at higher pressures, radiation from the ambient gas obscured spray details. Birk et al. [5] ignited the jet in 33-MPa, 500-C nitrogen from a particle bed heater and thus avoided the obscuration of the spray details by the ambient gas. They obtained excellent visual records of both the liquid jet and the flame structures, but practical considerations limited the maximum test pressure to 40-MPa maximum and the LP jets to 2-mm-diameter thickness. The present experimental approach is based on ballistic compression that provides 50 to 60 MPa of 850- to 1,000-C argon for ignition of 5-mm-thick LP jets. We concentrate here on the ballistic control of the experiment.

2. The Experimental Setup

2.1 Assembly of Major Components. The schematics of the setup and a sequence of its operation are depicted in Figure 1. A picture of the experimental facility is shown in Figure 2. The setup is comprised of a ballistic compressor interconnected in line with a liquid injector. The ballistic compressor consists of a gun and a test chamber that are interconnected via a piston-catching section (Figures 3 and 4). The gun is a modified 76-mm tank gun, M32, with a shortened barrel and bore machined smooth and chrome-plated, such that the inner diameter of both the barrel and the test section are 7.92 cm. The propelling charge is a small-grain M1 propellant (see Table 1) packed cylindrically around an M68 percussion primer in an M88B1 case (Figure 5). The firing pin activates pneumatically (Allenair electric-pneumatic solenoid Model V3MPA150). The barrel-breech assembly is anchored to a fixed stand, while the injector is fixed in multiple brackets that can slide (using Super Pillow Block Model SPB-16-OPN linear bearings) on two rod-like rails attached to the top of a wheeled screw-lift table (Lee Engineering Model P3060, 2,000-lb capacity). A hydraulic piston (Enerpac P-80, 50-ton capacity), placed between the injector and a fixed barrier (Figure 2), restrains the recoil of the ballistic compressor-injector. This arrangement allows for easy assembly and disassembly of the injector, test chamber, and piston-catching section. By wheeling the screw-lift table aside, the test chamber can be hoisted away, and access is provided to the muzzle of the gun for cleaning.

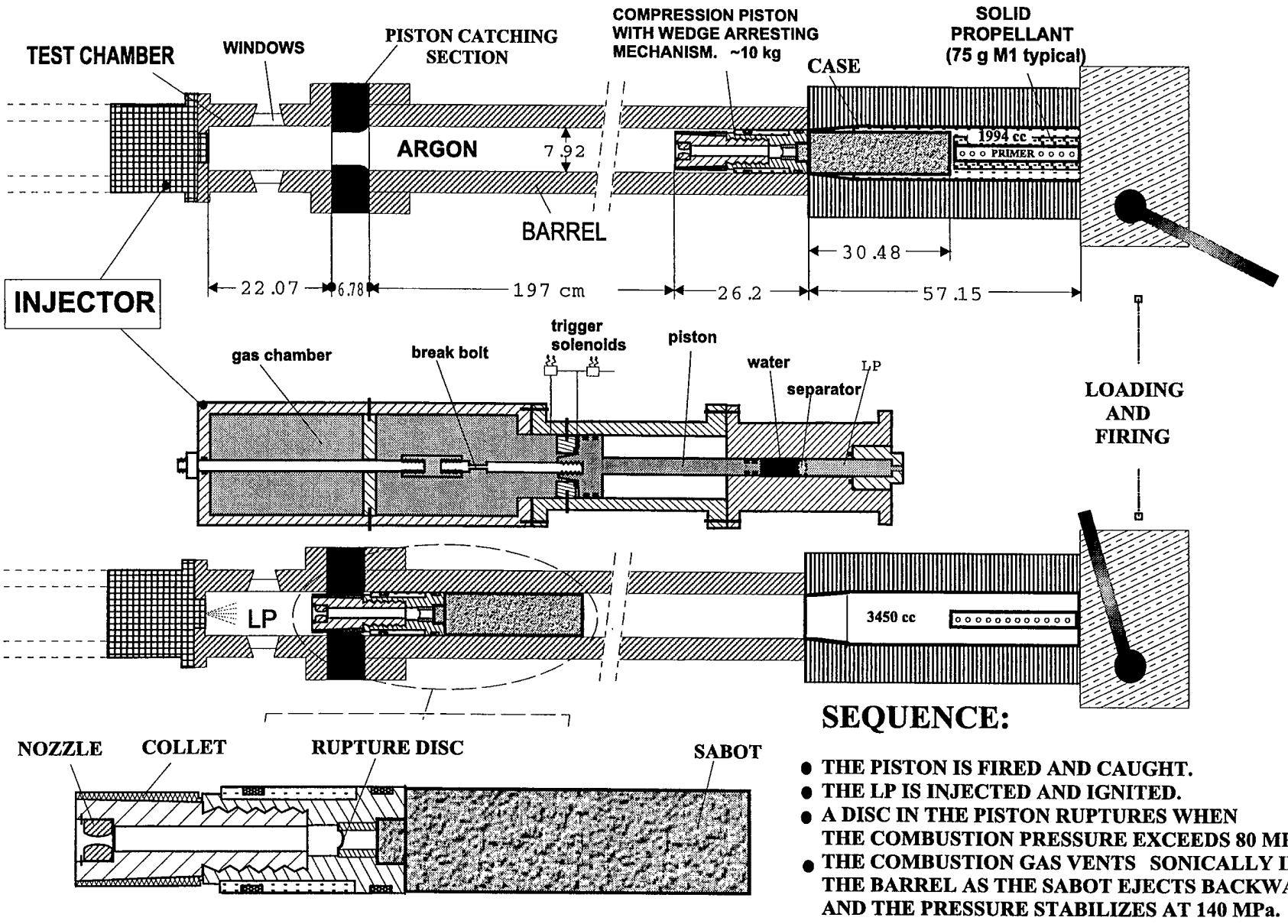

SEQUENCE:

- THE PISTON IS FIRED AND CAUGHT.
- THE LP IS INJECTED AND IGNITED.
- A DISC IN THE PISTON RUPTURES WHEN THE COMBUSTION PRESSURE EXCEEDS 80 MPa.
- THE COMBUSTION GAS VENTS SONICALLY INTO THE BARREL AS THE SABOT EJECTS BACKWARD, AND THE PRESSURE STABILIZES AT 140 MPa.

Figure 1. Schematic of the Experimental Setup and Sequence of Operations.

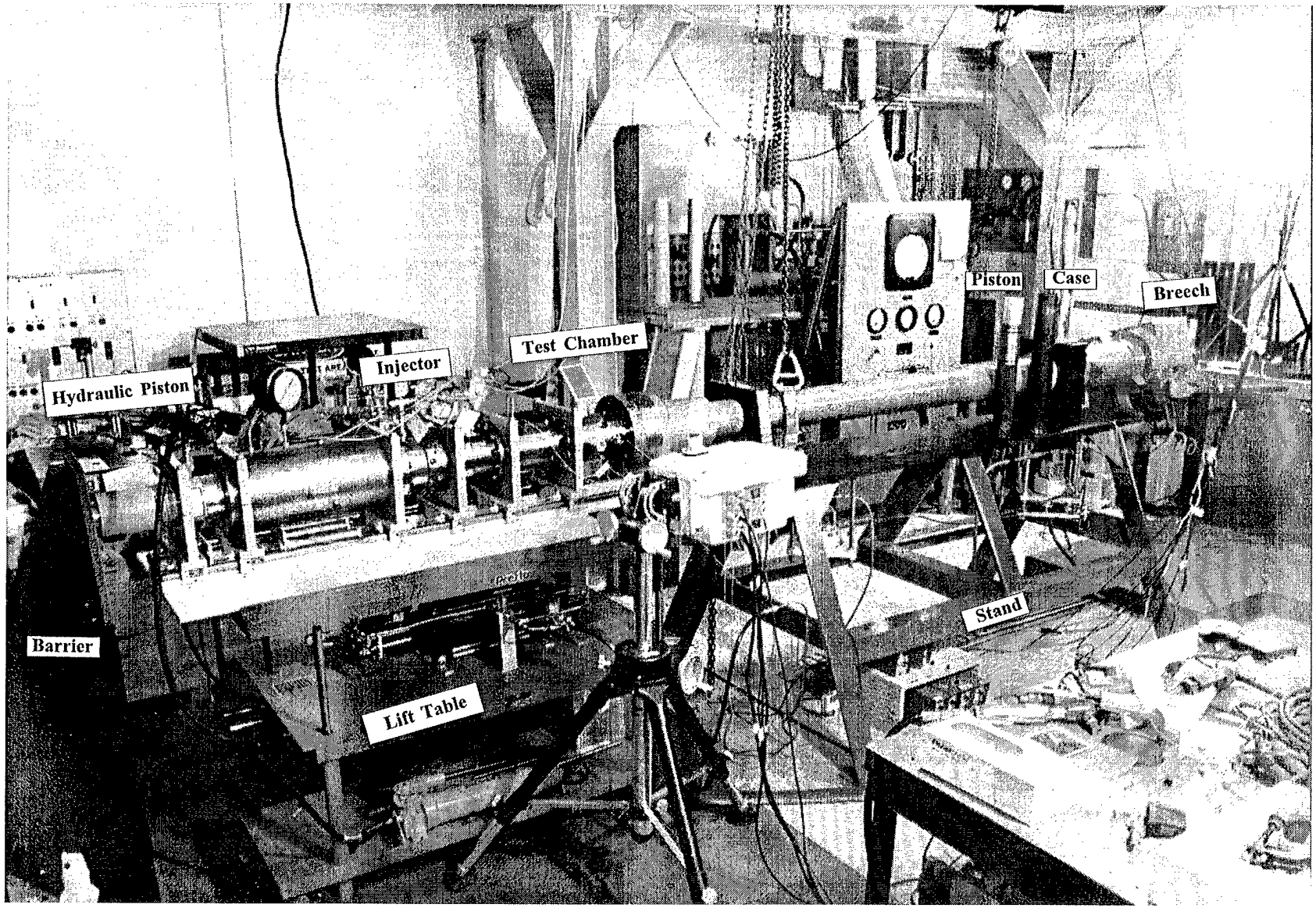

Figure 2. Picture of the Experimental Facility.

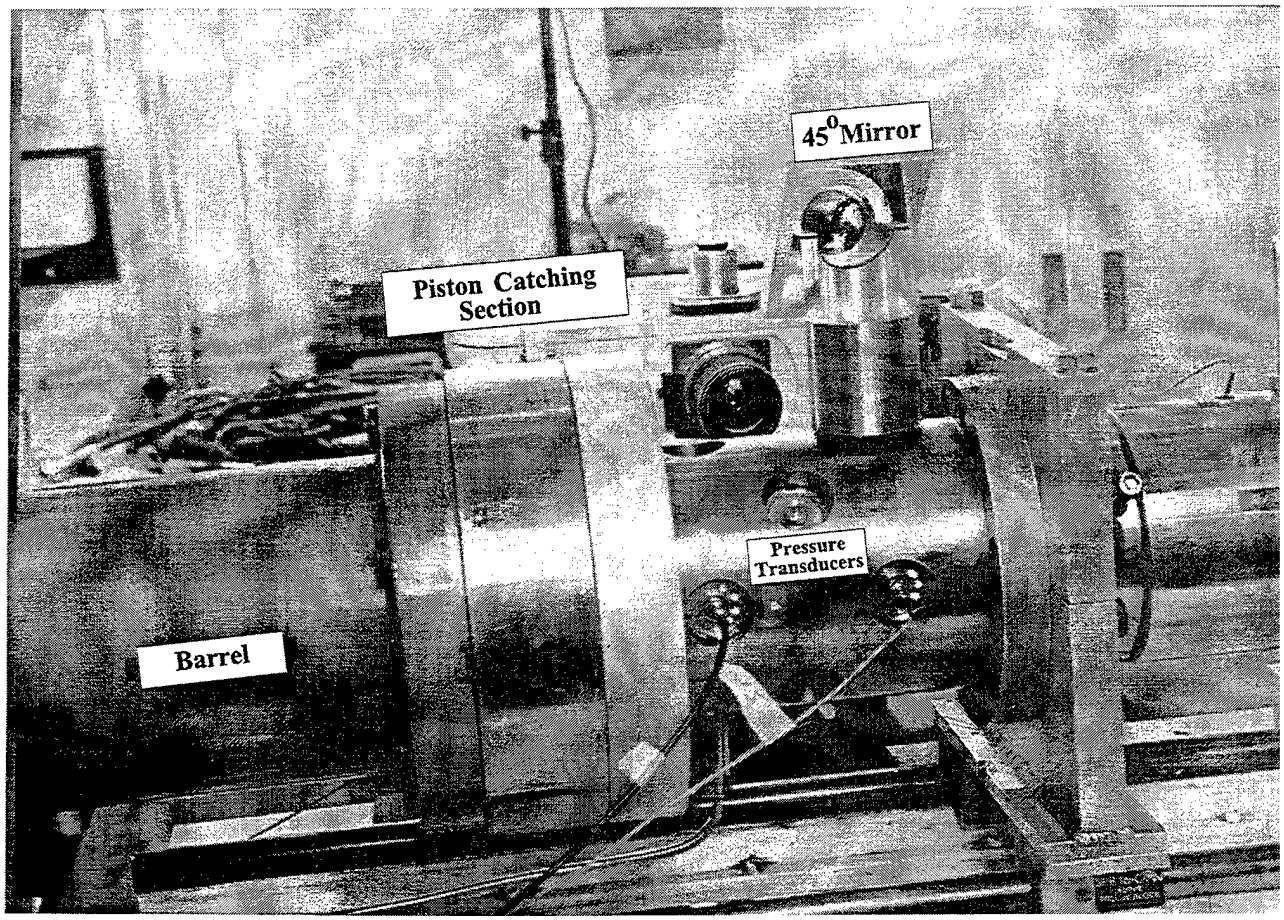

Figure 3. Side-View Picture of the Test Chamber and Piston-Catching-Section Connection to the Barrel.

2.2 The Piston. We denote the projectile a piston (see Figures 1, 2, 5 and 6). It comprises three main sections: sabot (rear), main body (center), and forward end. The sabot is made of phenolic, and, before the firing, it occupies the volume in the M88B1 case beyond the propellant charge and the primer. This effectively increases the loading density of the propellant so that it ignites promptly and burns efficiently. (Typically, the amount of propellant used is a small fraction of that used in the actual tank gun.) The main piston body contains the seals to the barrel's bore, and a rupture disk for pressure relief. The forward end of the piston is conically tapered with an angle of 3.14°

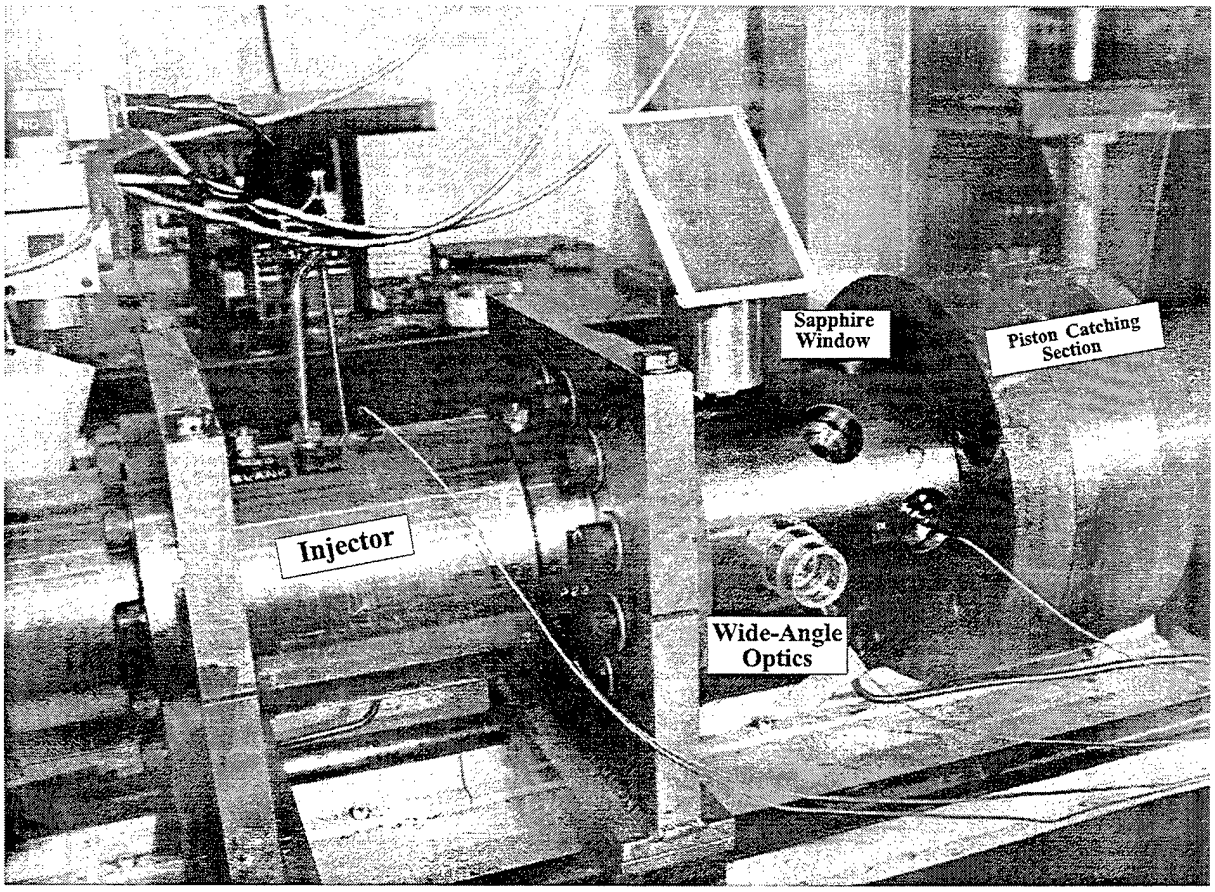

Figure 4. Side-View Picture of the Test Chamber Optics and Connections to the Piston-Catching Section and to the Injector.

(α=0.059) and fitted with a disposable collet made of 7075 T6 aluminum; it threads into the main body of the piston. The collet is 10.2 cm long and has four 0.32-cm-wide, 8.9-cm-long slots on each side. Its outer diameter is 7.29 cm and its inner diameters are 6.46 cm and 5.75 cm (α=0.059). The collet is machined to slide-fit into the catching section. The propelling charge and test gas pressure are chosen so that the front face of the piston enters 2 to 4 cm into the test chamber before attempting to rebound. The collet then locks between the catching section bore and the conical surface of the piston's forward end. This design is based on a wedge friction principle (see Figure 6). The post-test removal of the piston is shown in Figure 6.

Table 1. Input for the Simulations

Gun Chamber Volume (with projectile/sabot at initial position) = 1994 cm^3		Initial Gas Fill (90% argon, 10% air)	
Projectile		initial pressure	1.034 MPa (150 psi)
		molecular weight	38.6
projectile weight	10.092 kg	ratio of specific heats	1.61
projectile length	26.2 cm	covolume	0.688 cm^3/g
sabot length	30.34 cm		
Gun barrel length	223.2 cm	Propellant	
Length of piston-catching section	6.78 cm	Primer (black powder)	22 g
Test chamber length	22.07 cm	Solid propellant (M1)	75 g
Total possible travel	252.05 cm	burning rate (cm/s)	$0.1937[P(MPa)]^{0.7221}$
Propellant Geometry = single-perf. cylinder		Propellant Density = 1.569 g/cm^3	
		flame temperature	2417 Kelvin
grain length	0.5385 cm	impetus	923.6 J/g
grain diameter	0.1196 cm	ratio of specific heats	1.2593
perforation diameter	0.039878 cm	covolume	1.104 cm^3/g

2.3 The Test Chamber. The test chamber (Figure 3 and 4) is equipped with 12 modular window plugs that incorporate pressure transducers (Kistlers 607L and 607C2), sapphire-window inserts, and a gas port. The plugs are conical and sealed against the inner chamber wall by the chamber pressure. The sapphire windows are inserted in the plugs and sealed with epoxy. The windows are 13-mm thick and shaped as truncated cones with base diameters of 9.5 mm and 25 mm. The windows are rated for 250 MPa. Special optics were developed (under contract) for wide-angle viewing through the small-aperture (9.5-mm diameter) sapphire inserts. (See Figure 7 for details.) Figures 3 and 4 depict side views of the test chamber showing a Photec 16-mm high-speed framing camera trained through the wide-angle optics in position to photograph side-illuminated (via the 45° mirror) liquid jets inside the test chamber. (The mirror arrangement shown in Figure 7 is omitted in Figures 3 and 4.)

2.4 The Injector. The injector (Figures 1, 2, and 4) was built by the Sandia Combustion Research Facility (Livermore, CA) for earlier LP combustion experiments, and its adaptation to the

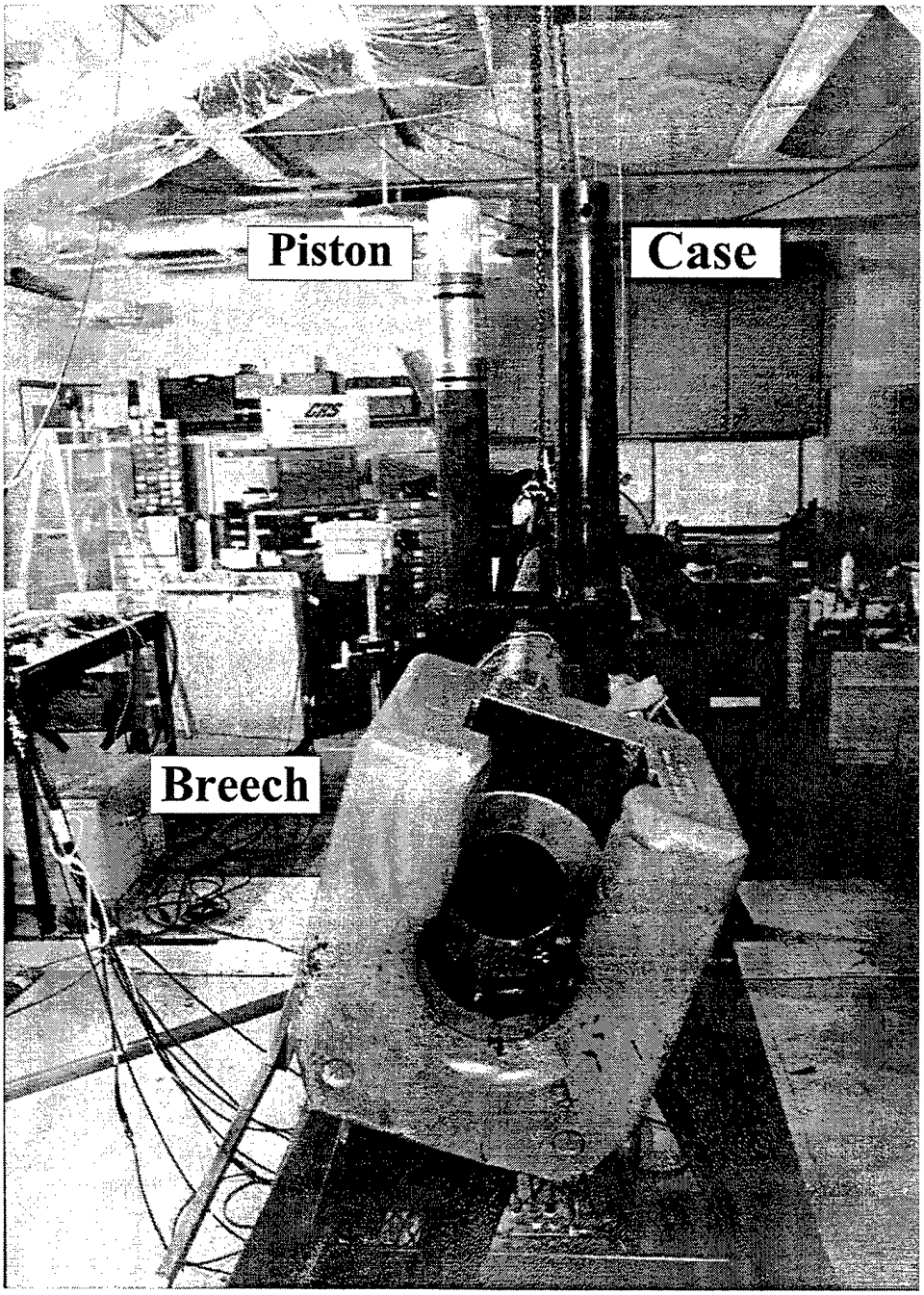

Figure 5. Rear-View Picture of the Open Breech, the Piston, and the Charge Case.

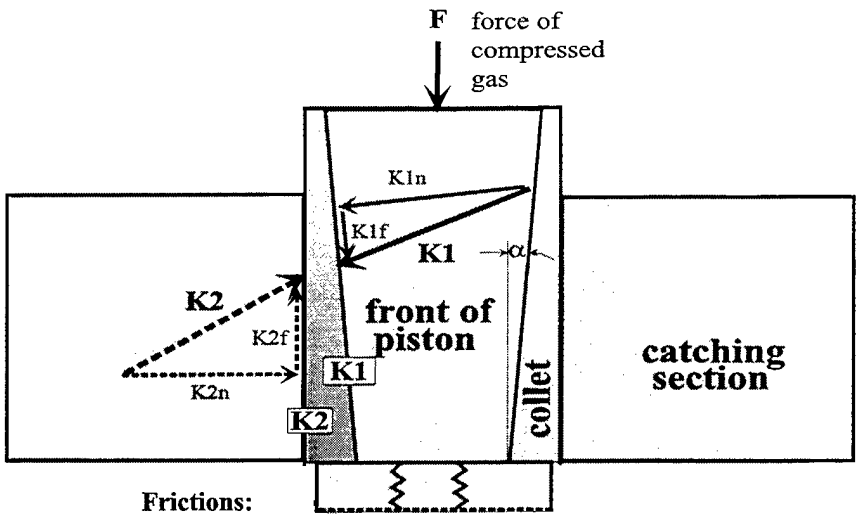

Frictions:

The friction coefficient on surface K1 is f1. **K1f = K1n * f1**
The friction coefficient on surface K2 is f2. **K2f = K2n * f2**

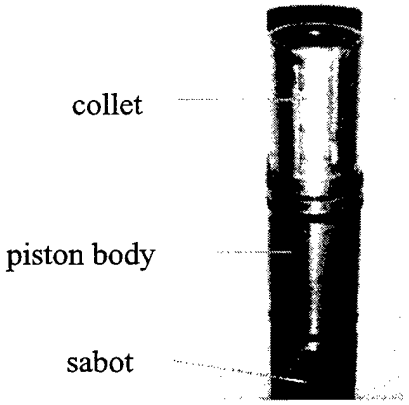

THE PISTON

FORCE POLYGON

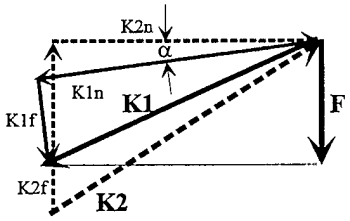

The collet locks if $\tan^{-1}$ f2 > α + $\tan^{-1}$ f1; therefore, f1 is made to be << f2

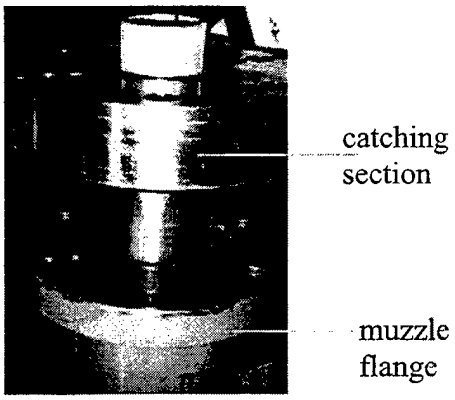

CATCHING SECTION AND CAUGHT PISTON BEING REMOVED FROM MUZZLE

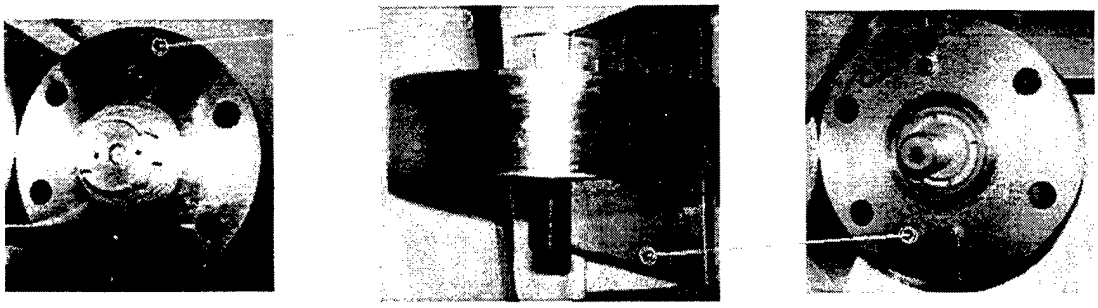

FRONT OF PISTON CAUGHT IN CATCHING SECTION

Figure 6. The Piston-Arrest Mechanism.

Optics Table Using *Beam 4–Optical Ray Tracer* Software

Refraction Index or Medium	x mm	1/ Radius of Curvature	Surface Identity	Diameter mm
1.00	0.00	0.0	Cgas	76.2
1.00	40.0	0.0	Lens	25.0
sapphire	53.0	0.0	Lens	9.5
1.00	55.0	0.0	Iris	7.5
1.00	56.0	0.0	Iris	7.5
1.00	57.24	-0.048193	Lens	10.0
BK7	58.74	0.048193	Lens	10.0
1.00	66.21	0.0	Lens	25.4
BK7	74.21	-0.064267	Lens	25.4
1.00	75.21	0.0	Lens	25.0
silica	77.21	0.028986	Lens	25.0
1.00	77.31	0.028727	Lens	30.0
1.67	88.31	-0.045208	Lens	30.0
1.67	88.311	-0.045208	Lens	30.0
1.728	90.51	-0.0049145	Lens	30.0
1.00	90.61	0.0	Lens	30.0
BK7	95.31	-0.0240964	Lens	30.0
1.00	95.41	0.0049145	Lens	30.0
1.728	97.51	0.045208	Lens	30.0
1.728	97.511	0.045208	Lens	30.0
1.67	108.51	-0.028727	Lens	30.0
1.00	110.66	-0.038565	Lens	30.0
BK7	112.66	0.0	Lens	30.0
1.00	154.50	0.0	FoPl	80

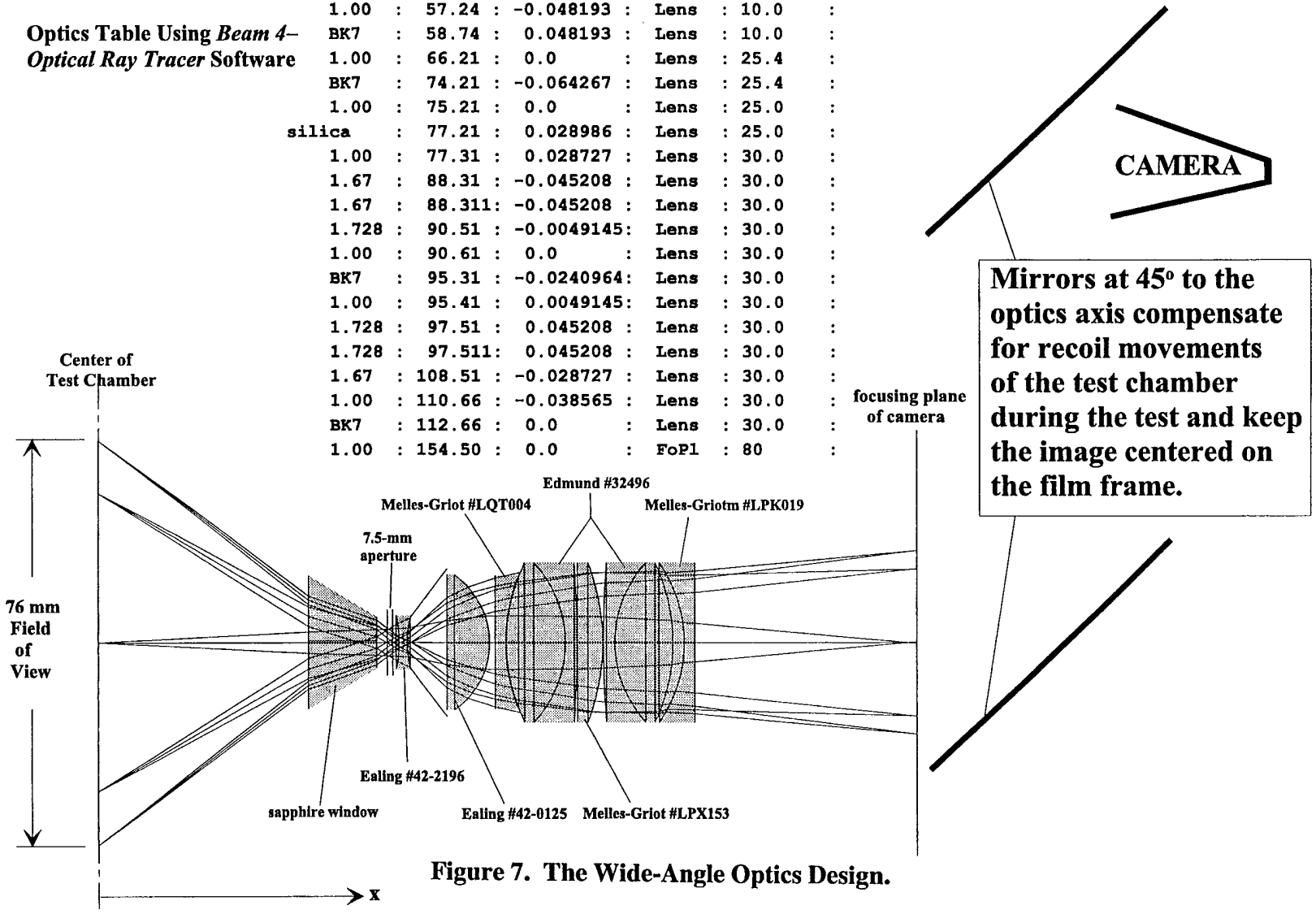

Figure 7. The Wide-Angle Optics Design.

present setup required only slight modifications. It operates autonomously by means of a differential area piston (i.e., the rear-facing surface is larger than the frontal surface). It features a sub-20-ms trigger time and typically injects 100-cm^3 LP in a circular 5-mm jet at over 300 m/s. The operation of the injector is as follows. The piston is pulled tight against the trigger section by the break-bolt assembly, such that an inner circle on the rear surface of the piston seals the gas chamber. The injector's orifice is sealed with an ejectable plastic plug to prevent liquid leakage. The injector's liquid chamber is filled with LP and water with a floating, collapsible plastic separator between the liquids. The LP is filled using a syringe, while the water is pressure-filled from a nitrogen-pressurized (3 MPa) accumulator. Ullage is bled through the filling ports on top of the injector. The gas chamber is pressurized with helium or nitrogen using a Haskel AGD62 air-driven gas booster compressor. The injector injects once the break-bolt breaks. This occurs when the trigger solenoids (Future Craft 203A8A-A-10) are activated and deliver the gas on the entire rear suface area of the piston. The liquid pressure in the injector is measured by two Kistler 607C2 pressure transducers. An example of liquid pressure in the injector is given in Figure 8. (The liquids on both sides of the separator were water, and the injector used 13.8-MPa nitrogen.) The upstream pressure transducer (P2) indicates when the front seals of the injection piston reach its location by a steep drop of its signal. The signal drop (to the test chamber pressure) from the downstream transducer (P1) indicates the end of the injection. Based on the injection pressures profiles and the positions of the front seal of the piston at the start and end of the piston's stroke, the average injection velocity can be easily calculated as shown in Figure 8.

2.5 Control of the Experiment and Data Acquisition. Handling of the test gas and the exhaust gas is done remotely using pneumatically operated stem valves (Autoclave 60VM4071-G4). The pneumatics are controlled using stacked solenoids (Humphrey S42E2). The test gas is filled through a gas port in a bottom window plug in the test chamber. The pressure is controlled using a high-resolution, 500-psi pressure gage (Heise C-62932). The combustion gas is vented from the breech section through a hole at the top of the case (Figure 5). The experiment is controlled via a timer sequencer (Special System 10-Stage programmer Model SSC-002-010). Two digital wave recorders (Nicolet Pro 20) are used for data acquisition.

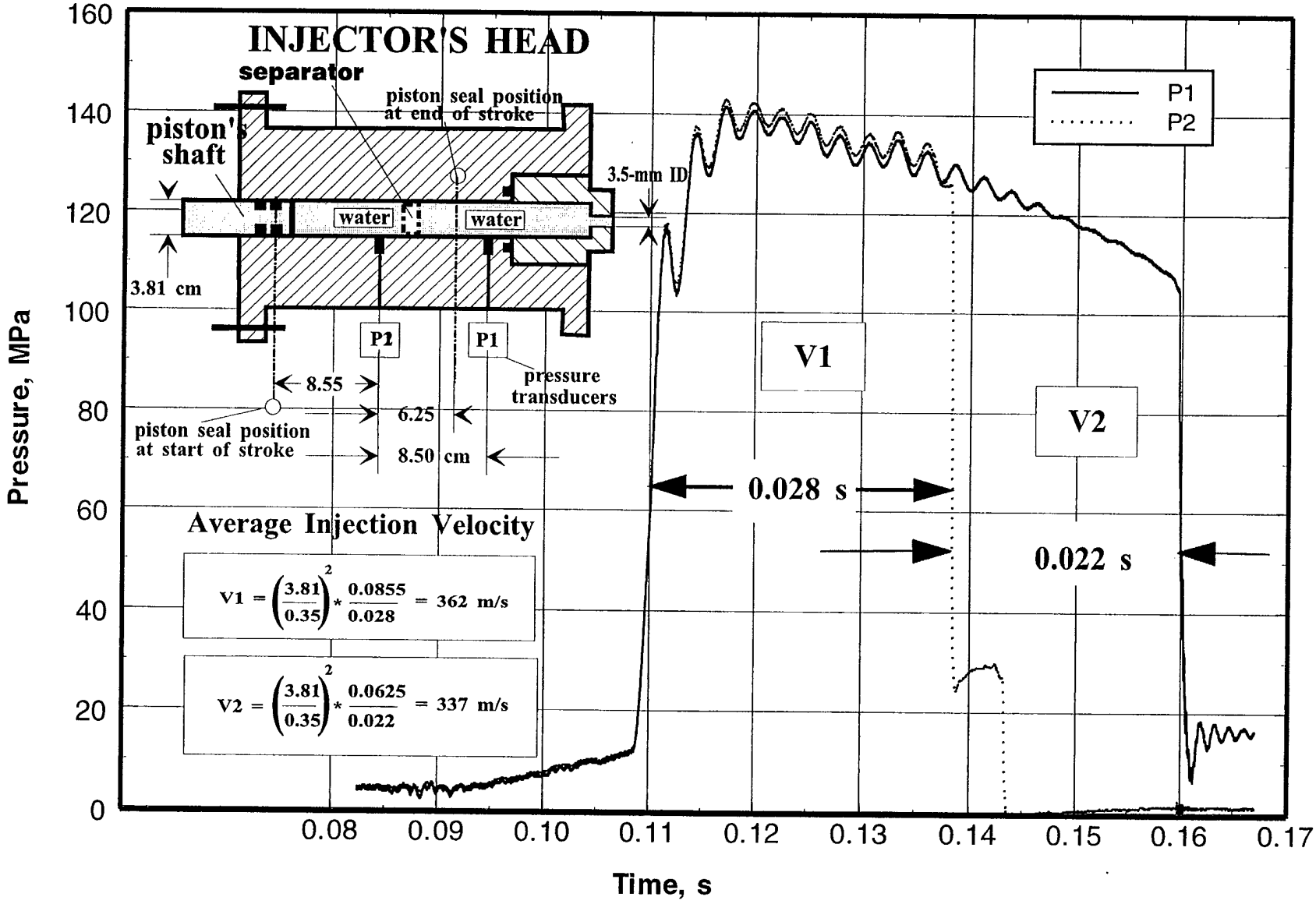

Figure 8. Example of Injector Pressures and Calculation of Injection Velocity.

2.6 Considerations in the Design of the Piston-Arrest Mechanism. The design of the piston-arrest mechanism is somewhat of an art. This is because the coefficients of friction (Figure 6) are not precisely known. Accordingly, the actual stresses in the collet can not be calculated. The collet holds against the test chamber pressure P by virtue of its shear stress with the catching-section wall. Because the ratio of the catching-section diameter to its length is approximately 1.1, the shear stress has to be at least $1.1P/4 = 35$ MPa for $P = 140$ MPa. This dictated the use of a metal-based collet rather than a plastic-based collet. Aluminum 7075-T6 was chosen because its ultimate yield strength is about 500 MPa, and, therefore, its shear strength is well over 100 MPa. The 7075-T6 tends to gall a steel surface— a phenomenon that results in a friction coefficient f2 well above 0.5. We achieve the locking condition specified in Figure 2 by greasing (with molybdenum-based grease) the surface between the collet and the front of the piston (i.e., $f1 << f2$), while keeping the surface between the collet and the catching section dry. To increase f2 we slightly knurled the locking surface of the catching section. The galling of the aluminum does not damage the underlying metal surfaces because the 7075-T6 aluminum alloy (150 Brinel hardness) is far softer than the 4043 steel alloy (45 Rockwell hardness) from which the front of the piston and the catching section are made.

Because the outer diameter of the collet is smaller than the barrel diameter, a volume of highly compressed gas is trapped momentarily around the collet between the front seal of the piston and the inlet to the piston-catching section when the collet enters the catching section. The pressure of this gas momentarily overshoots the test chamber pressure, but rapidly relaxes to the test chamber pressure via the slots in the collet. A stepped undercut on the back of the collet (Figure 1) provides area for the pressure overshoot to push the collet forward on the front of the piston, thus expanding the collet diameter and engaging it firmly onto the catching section.

Early versions of the piston-arrest mechanism did not include a special catching section. These designs experimented with collets made from phenolic and brass, which would lock the piston directly to the barrel without galling the chrome plating; however, the phenolic collet disengaged from the barrel wall when the differential pressure on the piston exceeded 5 MPa, and the brass collet disengaged above 10 MPa. Concern about potential damage to the chrome layer prompted the addition of the catching section, which allows use of aluminum collets and also facilitates dislodging the piston on completion of the test.

3. Numerical Simulation of the Ballistic Compressor

3.1 Model of Ballistic Compressor. A numerical model was constructed to simulate the transient flow field generated by the action of the ballistic compressor. The model consists of two separate elements linked by a shared boundary condition across the piston/projectile (see Figure 9). The lumped-parameter gun code "IBHVG2" [6] is used to describe the combustion of solid propellant in the chamber as well as flow in the gun tube up to the base of the piston. The initial condition assumes that the igniter material has been consumed and all propellant is ignited. The flow between the breech and the piston base is assumed quasi-steady with pressures dictated by the Lagrange gradient, which follows from a uniform density and a linear velocity profile.

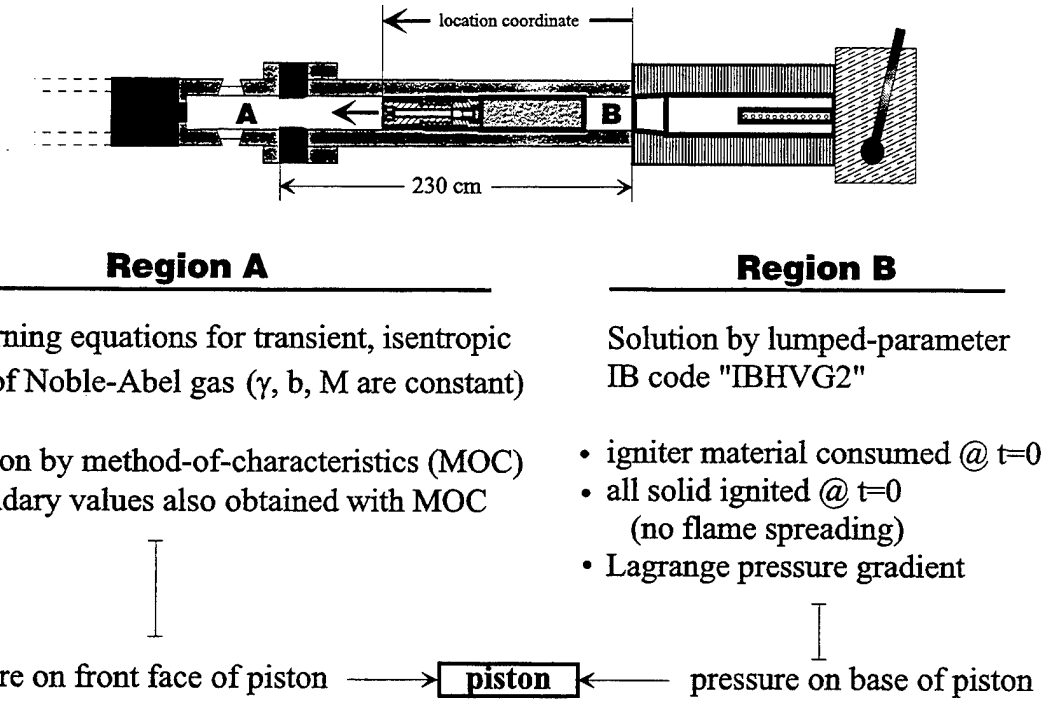

Figure 9. Synopsis of the Numerical Model.

The second element in the model is a description of the transient flow field between the forward end of the piston and the stationary, downstream wall of the test section. The time-dependent governing equations in this region assume isentropic flow of an Noble-Abel gas with constant molecular weight, covolume, and ratio of specific heats. With pressure P, density ρ, velocity u, and sound speed a, these equations can be written in characteristic form as

$$\frac{dP}{dt} \pm \rho a \frac{du}{dt} = 0 \ , \tag{1}$$

which are integrated, respectively, along the right (+) and left (−) running directions,

$$\frac{dz}{dt} = u \pm a \ , \tag{2}$$

and the energy equation

$$\frac{dP}{dt} - a^2 \frac{d\rho}{dt} = 0 \ , \tag{3}$$

which is integrated along the streamline

$$\frac{dz}{dt} = u \ . \tag{4}$$

When the coordinate system is in motion, the characteristic directions must be calculated with the velocity relative to the moving coordinate. With the temperature T, covolume b, ratio of specific heats γ, and gas constant $\Re$ ($\equiv$ universal gas constant/molecular weight), the Noble-Abel equation of state is simply

$$\frac{P}{\rho} = \frac{\Re T}{1 - \rho b} \ , \tag{5}$$

which dictates the sound speed

$$a^2 = \left.\frac{dP}{d\rho}\right|_{entropy} = \frac{\gamma P/\rho}{1 - \rho b} \quad . \tag{6}$$

Numerical solution of equations (1) and (3) is determined with the method-of-characteristics (MOC), which, to a great extent, will faithfully reproduce local wave motion and even propagate shock waves as discontinuities without spurious numerical oscillations. The MOC routines employed here were taken from Kooker [7], where all interpolation is done with Akima splines [8]. Boundary values are also obtained with special routines based on MOC. This solution procedure provides the value of pressure ahead of the projectile/piston, and IBHVG2 provides the value at the base. The net sum of these pressures, of course, controls the motion of the frictionless piston.

3.2 Sensitivity Analysis of Performance. The numerical simulation of the ballistic compressor was indispensable for determining operating conditions. The specifications and input values are summarized in Table 1. The parameters that influence performance are (1) test gas composition, (2) piston weight, (3) the propellant composition and geometry, (4) the initial test gas pressure, and (5) the mass of the propellant. The test gas composition was not varied in the simulation. Argon was chosen for the test gas because its high specific heat ratio yields a higher pressure ratio for the same volumetric compression ratio, and its high molecular weight leads to lower amplitude pressure waves upon compression. (The high-density argon is expected to aid in atomization and ignition of the LP jet. Practically, the argon is added to the atmospheric air in the compressor.) The piston weight was fixed in the simulation because the weight is practically imposed from structural and fabrication considerations; performance is more efficient with a heavier piston. The propellant composition was also fixed in the simulation. A fine grain M1 propellant was chosen because of its availability and efficient propulsion. The geometry of the fine grains provided the large surface area necessary for fast consumption of the propellant while the piston is still accelerating. The initial pressure of the test gas and the weight of the propellant can be easily controlled to affect performance. A baseline of 150 psi (1.034 MPa) of 10% air, 90 % argon, and 75-g M1, was found numerically and experimentally to provide the desired test chamber pressure and piston travel. The sensitivities of the pressure and travel to 20% variation in either initial gas pressure or propellant weight are shown in Figures 10 and 11. As expected, the test chamber pressure rises exponentially

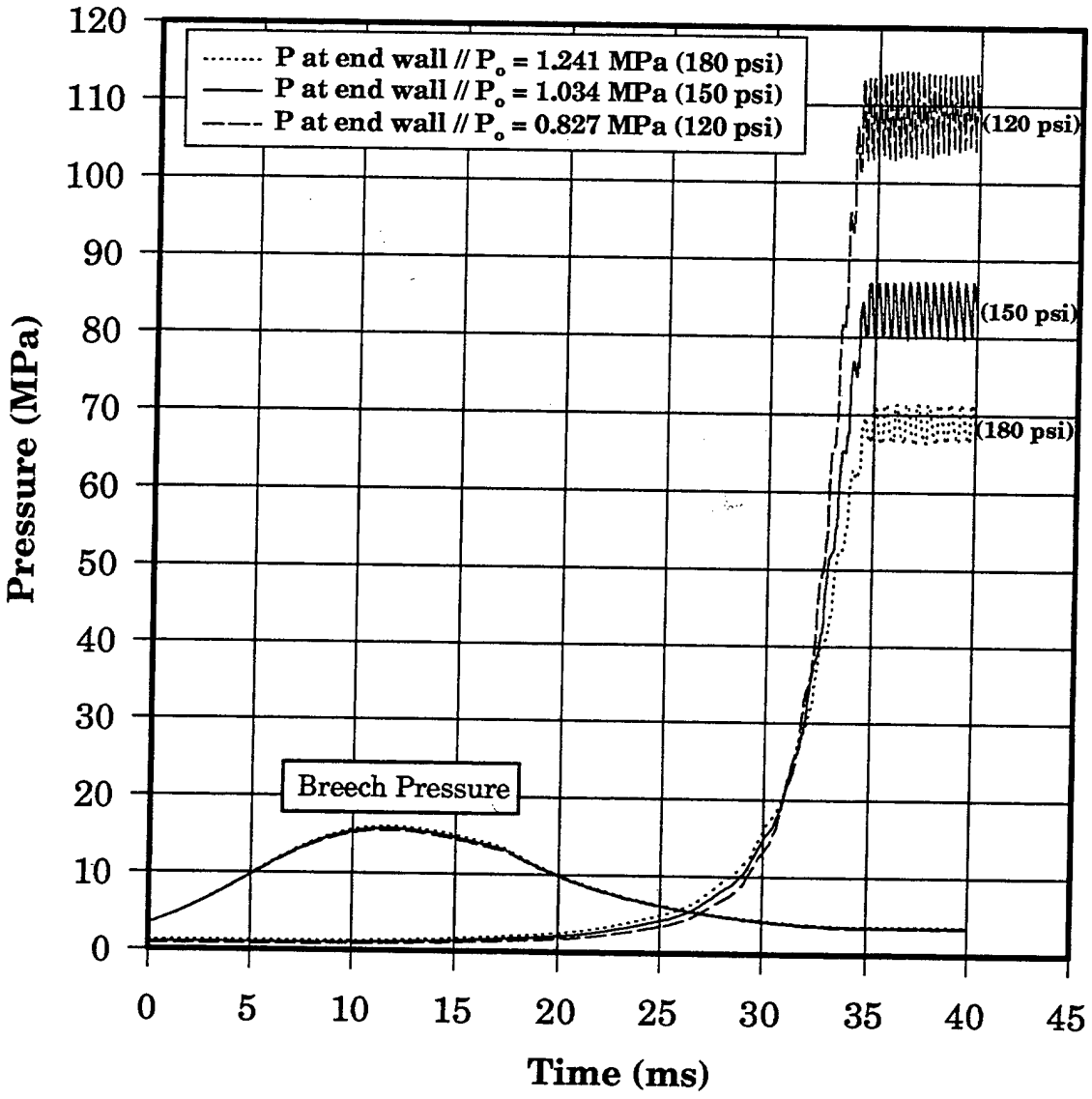

Figure 10. The Ballistic Compressor: Influence of Initial Pressure on Simulated Pressure-Time History at the Test Section End Wall. Initial Pressures are P_0 = 0.827 MPa, 1.034 MPa, and 1.241 Mpa; Piston Glides to Stop at Locations 239.1 cm, 234.9 cm, and 230.6 cm, Respectively. Charge Weight is 75 g of M1.

with time (i.e., piston travel), and larger amplitude pressure waves develop when the pressure rises are steeper. (In all the simulations, piston rebound is arrested.) Note that the maximum travel of the piston varies only 5 cm from the baseline value. The length of the catching section limits the experimental tolerance for successful catching of the piston to about 3% from baseline values of either the initial gas pressure or propellant weight.

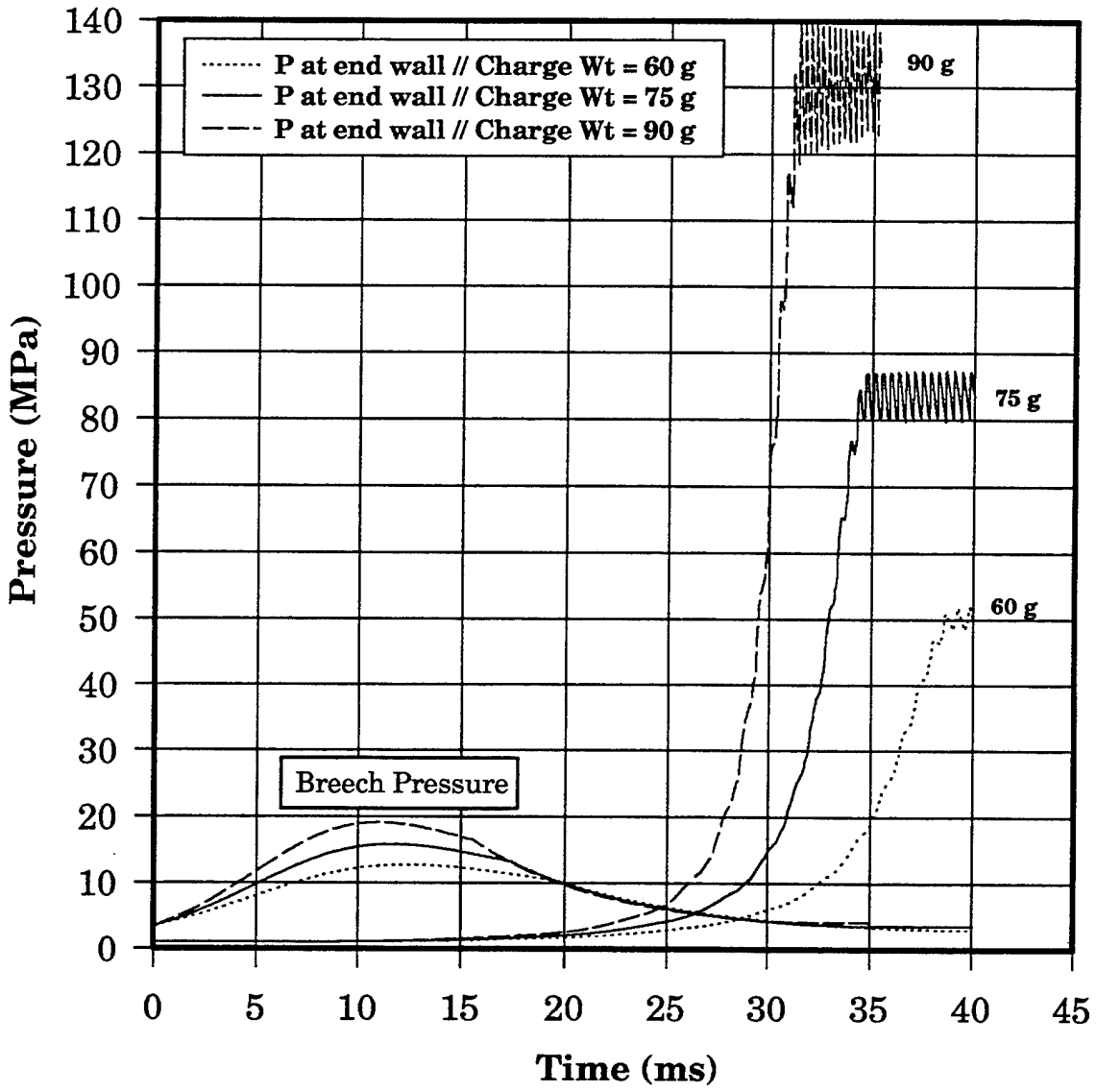

Figure 11. The Ballistic Compressor: Influence of M1 Charge Weight on Simulated Pressure-Time History at the Test Section End Wall. Charge Weighs are 60 g, 75 g, and 90 g; Piston Glides to a Stop at Locations 229.4 cm, 234.9 cm, and 238.4 cm, Respectively. P_o = 1.034 MPa (150 psi),

3.3 Experimental vs. Baseline Simulation. Figure 12 compares the simulated pressure-time histories at the test section end wall and gun breech with the experimental data. Figure 13 shows simulated time histories of piston velocity and location. The simulations assume the piston is arrested at the 234-cm distance because, in the experiment, the forward face of the piston traveled 234 cm from the entrance to the barrel (i.e., to 4 cm inside the test chamber) before rebound. In the

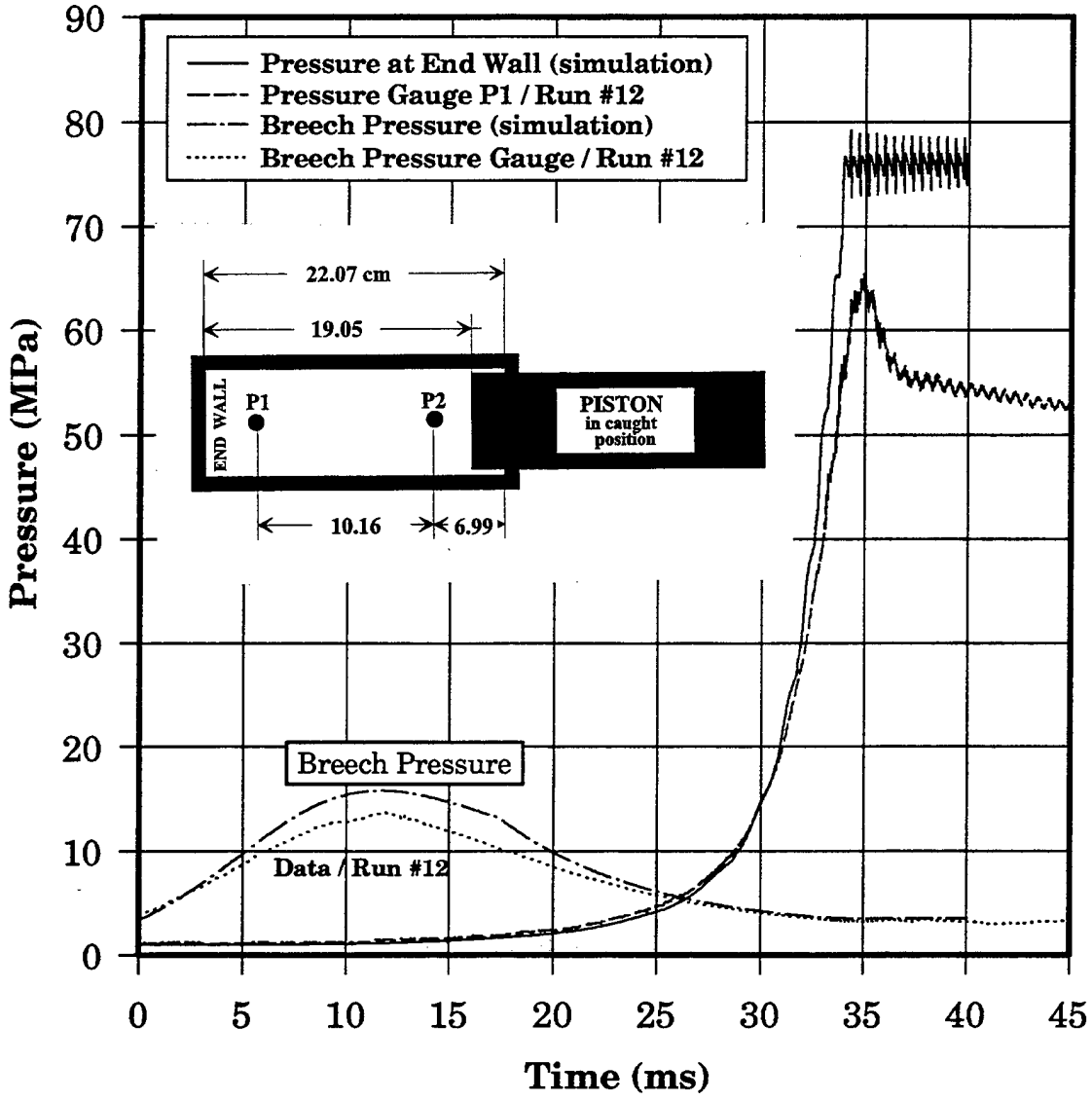

Figure 12. The Ballistic Compressor: M1 Charge Weight = 75 g, P_o = 1.034 MPa. Comparison of Simulated Pressure-Time History at Breech and Test Section End Wall With Data from Run no. 12 (Breech and P1 Transducers). Simulation Assumes Piston is Caught at 234 cm.

experiment, the piston rebound was arrested at the 233-cm distance. Two experiments were conducted, and their data vary less than 2% with respect to peak pressures and times. Comparison indicates the simulation is quite adequate, although the experimental breech and test chamber pressures, as well as the amplitude of the test chamber pressure waves, are lower than predicted. The shortfall in pressures is attributed to lower-than-expected actual propellant burn rate at the

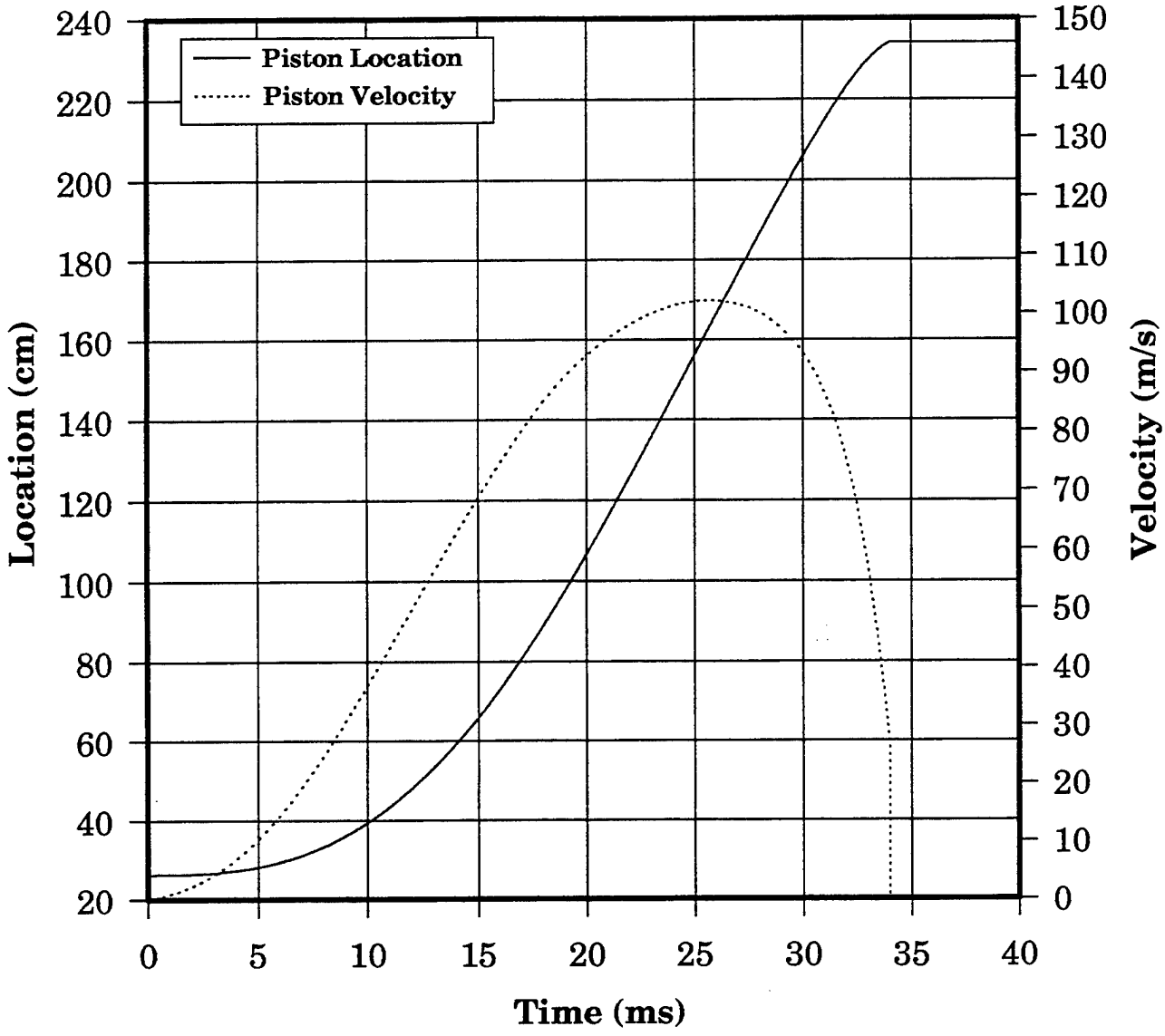

Figure 13. The Ballistic Compressor: Simulated Piston Velocity and Location as a Function of Time for Conditions of Run no. 12. M1 Charge Weight of 75 g, P_o = 1.034 MPa (150 psi). Simulation Assumes Piston is Caught at 234 cm.

sub-20-MPa breech pressure level. Additionally, the simulation does not account for heat losses ahead of the piston, nor does it account for viscous dissipation and deviation of the chamber walls from pure cylindrical (because of the window plugs). The heat losses cause the test chamber pressure to decrease gradually after the piston is caught, but there is a sufficiently long time interval of about 30 ms to effect LP jet ignition.

3.4 Test Chamber Temperature. The experimental test chamber temperature can be calculated by two independent methods, from the gas equation of state and from the sound speed. The gas density in the test chamber follows from the observed volumetric compression ratio (11.84) at the location where the piston was caught. Then from the gas equation of state (equation [5]) with a constant covolume of 0.688 cm^3/g, a chamber pressure of 55 MPa implies a temperature of 1,148 K. The basis for the second method is contained in the experimental pressure-time histories displayed in Figure 14, which give clear evidence for a standing wave in the test chamber once the piston is caught. The first longitudinal-mode wave pattern must be supported by a sound speed of 730 m/s. Substituting this value into the relationship for sound speed in equation (6) produces a temperature of 1,155 K (for pressure = 55 MPa). The two estimates of chamber temperatures agree well. Figure 15 is a plot of chamber temperature predicted by the numerical model as a function of pressure, with the average of the two experimental values at 55 MPa shown for comparison. As expected, the model that ignores heat losses ahead of the piston predicts a chamber temperature (1,350 K) that is a comfortable upper bound to the experimental value.

4. Summary

We constructed a novel ballistic compression facility for the visualization of the combustion of LP jets. The conditions for jet ignition are created by firing a piston toward a test chamber attached to the muzzle of a gun. Three system constraints were fixed at the outset: (1) the experiment is a failure unless the piston is caught, (2) the pressure level in the test section must be a minimum of 50 MPa when the piston motion is arrested, and (3) the weight (10 kg) of the piston is dictated by the requirements for mechanical/structural integrity in the ballistic environment. Under these conditions, the range of operating conditions is narrow. The ultimately successful mechanism that arrests the piston motion is a precision design with close tolerances. Model predictions were an invaluable guide in making decisions about allowable initial conditions; a successful catch required accurate predictions of piston location and velocity at the end of the cycle. We have achieved excellent ballistic control of the experiment.

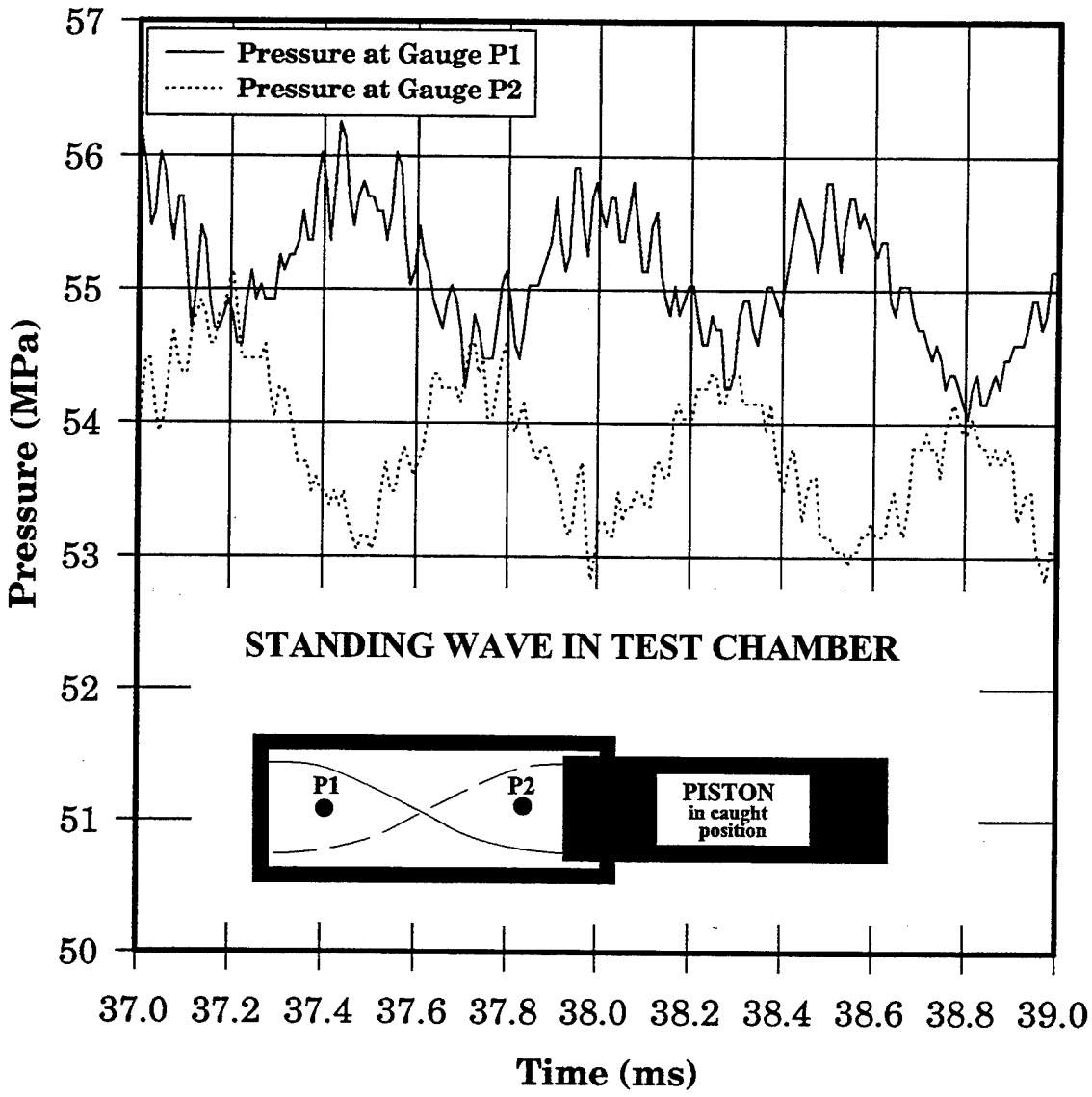

Figure 14. The Ballistic Compressor: Data From Run no. 12, Time History From 37–39 ms From Pressure Transducers P1 and P2. Evidence for Standing Wave in Test Section.

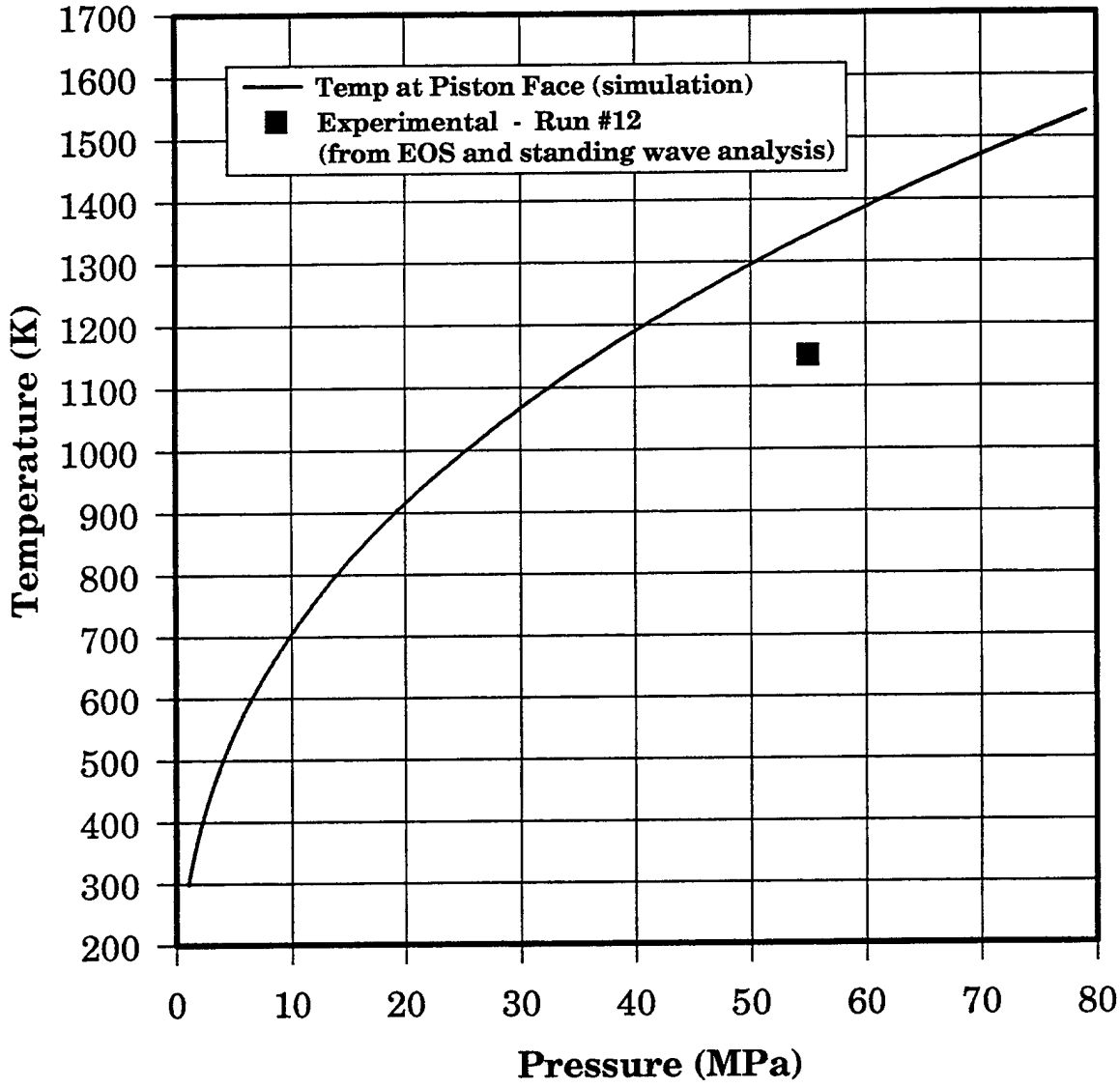

Figure 15. The Ballistic Compressor: Simulated Gas Temperature as a Function of Pressure at the Piston Face for Condition of Run no. 12. Datum is Experimental Value Deduced from (a) Equation of State for P = 55 MPa and (b) Properties of Standing-Wave Cycle (Figure 14).

INTENTIONALLY LEFT BLANK.

5. References

1. Morrison, W. F., J. D. Knapton, and M. J. Bulman. "Liquid Propellant Guns." *Gun Propulsion Technology,* vol. 109, chap. 13, pp. 413–471, *Progress in Astronautics and Aeronautics*, L. Stiefel (ed.) AIAA, Washington, DC, 1988.

2. Baier, G. R., "Analytical and Experimental Analysis of Liquid Propellant Injection and Ignition at High Pressures." Master of Engineering Dissertation, Renseselaer Polytechnic Institute, Troy, NY, 1986.

3. Birk, A., and P. Reeves. "Annular Liquid Propellant Jets—Injection, Atomization, and Ignition." BRL-TR-2780, U.S. Army Ballistic Research Laboratory, Aberdeen Proving Ground, MD, March 1987.

4. Lee, T.-W., L. -K. Tseng, and G. M. Faeth. " Separated Flow Considerations for Pressure Atomized Combusting Monopropellant Sprays." *J. Prop. Power*, vol. 6, no. 4, pp. 382–391, 1990.

5 Birk, A., and M. McQuaid. "Combustion of Han-Based Liquid Propellant Sprays at 28–38 MPa." *Combustion Science and Technology*, vol. 106, pp. 1–17, 1995.

6. Anderson, R. D., and K. D. Fickie. "IBHVG2A User's Guide." BRL-TR-2829, U.S. Army Ballistic Research Laboratory, Aberdeen Proving Ground, MD, July 1987.

7. Kooker, D. E. "Modeling of Compaction Wave Behavior in Confined Granular Energetic Material." BRL-TR-3138, U.S. Army Ballistic Research Laboratory, Aberdeen Proving Ground, MD, August 1990.

8. IMSL. "User's Manual/Math Library." Ver 1.1, Houston, Texas, 1989. (For Akima splines, see p. 420)

INTENTIONALLY LEFT BLANK.

NO. OF COPIES	ORGANIZATION
2	DEFENSE TECHNICAL INFORMATION CENTER DTIC DDA 8725 JOHN J KINGMAN RD STE 0944 FT BELVOIR VA 22060-6218
1	HQDA DAMO FDQ DENNIS SCHMIDT 400 ARMY PENTAGON WASHINGTON DC 20310-0460
1	CECOM SP & TRRSTRL COMMCTN DIV AMSEL RD ST MC M H SOICHER FT MONMOUTH NJ 07703-5203
1	PRIN DPTY FOR TCHNLGY HQ US ARMY MATCOM AMCDCG T M FISETTE 5001 EISENHOWER AVE ALEXANDRIA VA 22333-0001
1	PRIN DPTY FOR ACQUSTN HQS US ARMY MATCOM AMCDCG A D ADAMS 5001 EISENHOWER AVE ALEXANDRIA VA 22333-0001
1	DPTY CG FOR RDE HQS US ARMY MATCOM AMCRD BG BEAUCHAMP 5001 EISENHOWER AVE ALEXANDRIA VA 22333-0001
1	DPTY ASSIST SCY FOR R&T SARD TT T KILLION THE PENTAGON WASHINGTON DC 20310-0103
1	OSD OUSD(A&T)/ODDDR&E(R) J LUPO THE PENTAGON WASHINGTON DC 20301-7100

NO. OF COPIES	ORGANIZATION
1	INST FOR ADVNCD TCHNLGY THE UNIV OF TEXAS AT AUSTIN PO BOX 202797 AUSTIN TX 78720-2797
1	DUSD SPACE 1E765 J G MCNEFF 3900 DEFENSE PENTAGON WASHINGTON DC 20301-3900
1	USAASA MOAS AI W PARRON 9325 GUNSTON RD STE N319 FT BELVOIR VA 22060-5582
1	CECOM PM GPS COL S YOUNG FT MONMOUTH NJ 07703
1	GPS JOINT PROG OFC DIR COL J CLAY 2435 VELA WAY STE 1613 LOS ANGELES AFB CA 90245-5500
1	ELECTRONIC SYS DIV DIR CECOM RDEC J NIEMELA FT MONMOUTH NJ 07703
3	DARPA L STOTTS J PENNELLA B KASPAR 3701 N FAIRFAX DR ARLINGTON VA 22203-1714
1	SPCL ASST TO WING CMNDR 50SW/CCX CAPT P H BERNSTEIN 300 O'MALLEY AVE STE 20 FALCON AFB CO 80912-3020
1	USAF SMC/CED DMA/JPO M ISON 2435 VELA WAY STE 1613 LOS ANGELES AFB CA 90245-5500

NO. OF
COPIES ORGANIZATION

1 US MILITARY ACADEMY
MATH SCI CTR OF EXCELLENCE
DEPT OF MATHEMATICAL SCI
MDN A MAJ DON ENGEN
THAYER HALL
WEST POINT NY 10996-1786

1 DIRECTOR
US ARMY RESEARCH LAB
AMSRL CS AL TP
2800 POWDER MILL RD
ADELPHI MD 20783-1145

1 DIRECTOR
US ARMY RESEARCH LAB
AMSRL CS AL TA
2800 POWDER MILL RD
ADELPHI MD 20783-1145

3 DIRECTOR
US ARMY RESEARCH LAB
AMSRL CI LL
2800 POWDER MILL RD
ADELPHI MD 20783-1145

ABERDEEN PROVING GROUND

3 DIR USARL
AMSRL CI LP (305)

NO. OF COPIES	ORGANIZATION
2	COMMANDER US ARMY ARDEC AMSTA AR AEE B D DOWNS AMSTA AR FSS DA J IRIZARRY PICATINNY ARSENAL NJ 07805-5000
2	COMMANDER US ARMY ARDEC AMSTA AR AEE A BRACUTI D CHIU PICATINNY ARSENAL NJ 07806-5000
1	DIRECTOR AMXRO MCS DR D MANN PO BOX 12211 RESEARCH TRIANGLE PARK NC 27709-2211
1	DIRECTOR AMXRO RT IP LIB SER PO BOX 12211 RESEARCH TRIANGLE PARK NC 27709-2211
1	OLAC PL RKFA D TALLEY EDWARDS AFB CA 93524
1	CA INST OF TECHNOLOGY JET PROPULSION LAB TECH LIB 4800 OAK GROVE DR PASADENA CA 91109-8099
1	THE PENN STATE UNIV PROF K KUO 140 RESEARCH BLDG E BIGLER RD UNIVERSITY PARK PA 16802-7501

NO. OF COPIES	ORGANIZATION
2	DIRECTOR JET PROPULSION LAB J BELLAN D MAYNARD 4800 OAK GROVE DR PASADENA CA 91109-8099
1	VEHICLE PROPULSION DIR NASA LEWIS RSRCH CTR MS 603 TECH LIB 21000 BROOKPARK RD CLEVELAND OH 44135-3191
1	DIRECTOR SANDIA NATL LABS R CARLING DIV 8357 PO BOX 696 LIVERMORE CA 94551-0969
1	DIRECTOR THE JOHNS HOPKINS UNIV APPLIED PHYSICS LAB JOHNS HOPKINS RD LAUREL MD 20707
1	PAUL GOUGH ASSOC INC DR P GOUGH 1048 SOUTH ST PORTSMOUTH NH 03801-5423
2	JOHNS HOPKINS UNIV CPIA T CHRISTIAN TECH LIB 10630 LITTLE PATUXENT PKWY STE 202 COLUMBIA MD 21042-3200
3	GENERAL DYNAMICS DEF SYS CO INDER MAGOON T KURIATA B FETHEROLF 100 PLASTICS AVE PITTSFIELD MA 01201

NO. OF
COPIES ORGANIZATION

2 PRINCETON CMBSTN RSCH LAB
M TARCZYNSKI
N MESSINA
PRINCETON CORP PLAZA
11 DEERPARK DR
BLDG IV STE 119
MONMOUTH JUNCTION NJ 08852

ABERDEEN PROVING GROUND

34 DIR, USARL
AMSRL WM P
A HORST
AMSRL WM PA
A BIRK (10 CPS)
L-M CHANG
T COFFEE
P CONROY
J COLBURN
J DE SPIRITO
A JUHASZ
G KELLER
J KNAPTON
D KOOKER
C LEVERITT
M MCQUAID
T MINOR
M NUSCA
W OBERLE
T ROSENBERGER
K WHITE
G WREN
AMSRL WM PB
P PLOSTINS
AMSRL WM PC
R BEYER
B FORCH
M MILLER
J VANDERHOFF
AMSRL WM PD
B BURNS

REPORT DOCUMENTATION PAGE

Form Approved
OMB No. 0704-0188

Public reporting burden for this collection of information is estimated to average 1 hour per response, including the time for reviewing instructions, searching existing data sources, gathering and maintaining the data needed, and completing and reviewing the collection of information. Send comments regarding this burden estimate or any other aspect of this collection of information, including suggestions for reducing this burden, to Washington Headquarters Services, Directorate for Information Operations and Reports, 1215 Jefferson Davis Highway, Suite 1204, Arlington, VA 22202-4302, and to the Office of Management and Budget, Paperwork Reduction Project(0704-0188), Washington, DC 20503.

1. AGENCY USE ONLY *(Leave blank)*	2. REPORT DATE	3. REPORT TYPE AND DATES COVERED
	September 1997	Final, Oct 95-Sep 96

4. TITLE AND SUBTITLE
A Ballistic Compressor-Based Setup for the Visualization of Liquid Propellant Jet Combustion Above 100 MPa

5. FUNDING NUMBERS
1L1622618AH37

6. AUTHOR(S)
Avi Birk and Douglas E. Kooker

7. PERFORMING ORGANIZATION NAME(S) AND ADDRESS(ES)
U.S Army Research Laboratory
ATTN: AMSRL-WM-PA
Aberdeen Proving Ground, MD 21005-5066

8. PERFORMING ORGANIZATION REPORT NUMBER
ARL-TR-1490

9. SPONSORING/MONITORING AGENCY NAMES(S) AND ADDRESS(ES)

10.SPONSORING/MONITORING AGENCY REPORT NUMBER

11. SUPPLEMENTARY NOTES

12a. DISTRIBUTION/AVAILABILITY STATEMENT
Approved for public release; distribution is unlimited.

12b. DISTRIBUTION CODE

13. ABSTRACT *(Maximum 200 words)*

This report describes the components and operation of an experimental setup for the visualization of liquid propellant (LP) jet combustion at pressures above 100 MPa. The apparatus consists of an in-line ballistic compressor and LP injector. The ballistic compressor, based on a modified 76-mm gun, provides high-pressure (55 MPa) clear hot gas for the jet ignition. A piston (projectile) is fired toward a test chamber beyond the barrel's end, and its rebound is arrested in a transition section between the test chamber and the barrel. The LP jet is injected once the piston is restrained, and combustion of the jet further elevates the pressure. At a preset pressure, a disk in the piston ruptures, and the combustion gas vents sonically into the barrel. If a monopropellant is used, the jet injection-combustion process then resembles liquid rocket combustion, but at very high pressures (140 MPa). This report discusses the ballistics of the compression and compares experimental results to those predicted by a numerical model of the apparatus. Experimentally, a pressure of 70 MPa was achieved upon a 12.5 volumetric compression factor by firing a 10-kg piston into 1.04-MPa argon, using a charge of 75 g of small-grain M1 propellant.

14. SUBJECT TERMS
ballistic compressor, high-pressure spray combustion, liquid jet, liquid propellant

15. NUMBER OF PAGES
34

16. PRICE CODE

17. SECURITY CLASSIFICATION OF REPORT	18. SECURITY CLASSIFICATION OF THIS PAGE	19. SECURITY CLASSIFICATION OF ABSTRACT	20. LIMITATION OF ABSTRACT
UNCLASSIFIED	UNCLASSIFIED	UNCLASSIFIED	UL

NSN 7540-01-280-5500
Standard Form 298 (Rev. 2-89)
Prescribed by ANSI Std. 239-18 298-102

INTENTIONALLY LEFT BLANK.

USER EVALUATION SHEET/CHANGE OF ADDRESS

This Laboratory undertakes a continuing effort to improve the quality of the reports it publishes. Your comments/answers to the items/questions below will aid us in our efforts.

1. ARL Report Number/Author ARL-TR-1490 (Birk) Date of Report September 1997

2. Date Report Received _____

3. Does this report satisfy a need? (Comment on purpose, related project, or other area of interest for which the report will be used.) _____

4. Specifically, how is the report being used? (Information source, design data, procedure, source of ideas, etc.) _____

5. Has the information in this report led to any quantitative savings as far as man-hours or dollars saved, operating costs avoided, or efficiencies achieved, etc? If so, please elaborate. _____

6. General Comments. What do you think should be changed to improve future reports? (Indicate changes to organization, technical content, format, etc.) _____

CURRENT ADDRESS

_____
Organization

_____
Name E-mail Name

_____
Street or P.O. Box No.

_____
City, State, Zip Code

7. If indicating a Change of Address or Address Correction, please provide the Current or Correct address above and the Old or Incorrect address below.

OLD ADDRESS

_____
Organization

_____
Name

_____
Street or P.O. Box No.

_____
City, State, Zip Code

(Remove this sheet, fold as indicated, tape closed, and mail.)

(DO NOT STAPLE)

DEPARTMENT OF THE ARMY

OFFICIAL BUSINESS

NO POSTAGE
NECESSARY
IF MAILED
IN THE
UNITED STATES

BUSINESS REPLY MAIL
FIRST CLASS PERMIT NO 0001,APG,MD

POSTAGE WILL BE PAID BY ADDRESSEE

DIRECTOR
US ARMY RESEARCH LABORATORY
ATTN AMSRL WM PB
ABERDEEN PROVING GROUND MD 21005-5066